

Numerical study of energy dissipation and block barriers in stepped spillways

Mehdi Karami Moghadam, Ata Amini and Ehsan Karami Moghadam

ABSTRACT

In this research, the accuracy of the Flow-3D numerical model in the flow simulation in a stepped spillway was probed using data obtained from the physical model. In addition, the effects of block barriers on the energy dissipation rate were investigated. To adopt a proper turbulent model, Renormalization Group $k-\epsilon$, RNG $k-\epsilon$, and standard $k-\epsilon$ models were employed. Then, the Flow-3D was run in five discharges for nine spillways with the ratios of block length to step length (L_b/l) and block height to step height (H_b/h) as 0.3, 0.4, and 0.5. The results indicated that both turbulent models had almost similar outcomes though the run time of the RNG $k-\epsilon$ model was shorter. The blocks with a shorter length in low ratios of H_b/h and the lengthier blocks in high ratios of H_b/h undergo more relative energy dissipation relative to the no-block situation. For $H_b/h = 0.3$ and L_b/l equal to 0.3, 0.4, and 0.5, the relative energy dissipation climbed on average as 8.5, 6.5, and 4.5% respectively, compared with the no-block case. The most influence exerted on relative energy dissipation was obtained via the blocks with $H_b/h = L_b/l$ equal to 0.3 and 0.5 with respective increases of 8.6 and 8.4%.

Key words | energy dissipation, nappe flow, skimming flow, stepped spillway

Mehdi Karami Moghadam
Department of Agriculture,
Payame Noor University (PNU),
Tehran,
Iran

Ata Amini (corresponding author)
Kurdistan Agricultural and Natural Resources
Research and Education Center, AREEO,
Sanandaj,
Iran
E-mail: a.amini@areeo.ac.ir

Ehsan Karami Moghadam
Department of Civil Engineering,
Shahid Bahonar University,
Kerman,
Iran

HIGHLIGHTS

- The Flow-3D model applied to examine the effects of height and length of the block on the energy dissipation.
- As the discharge increases, the energy dissipation decreases and the effects of blocks increases.
- Shorter blocks at lower elevations and longer blocks at higher length had the highest energy dissipation.
- The blocks with length/height equal to 0.3 and 0.5 were assigned the most increase in energy dissipation.

NOTATION

The following symbols are used in this paper:

\bar{P} average dissipation of energy in Flow-3D
 \bar{O} average dissipation of energy in the physical model
 EL_c spillway's crest level at upstream proportionate to the flume's bottom at downstream

Fr Froude Number
 g gravitational acceleration
 h step's height
 H_1 energy at the spillway's toe
 H_b height of the block
 H_t total energy of flow at the spillway's upstream
 l step's length
 L_b block's length
 n number of data

This is an Open Access article distributed under the terms of the Creative Commons Attribution Licence (CC BY 4.0), which permits copying, adaptation and redistribution, provided the original work is properly cited (<http://creativecommons.org/licenses/by/4.0/>).

doi: 10.2166/hydro.2020.245

N	number of steps
O_j	energy dissipation rate in the physical model
P_0	pressure (absolute) at some reference point in the flow
P_1	amount of energy dissipation in model Flow-3D
P_v	water vapor pressure (absolute)
q	unit discharge
Re	Reynolds Number
V_0	flow velocity
y	upstream flow depth
y_1	primary depth of hydraulic jump
y_2	sequent depth of the hydraulic jump
y_c	critical depth
ΔH	energy difference between upstream and downstream
$\Delta H/H_t$	relative energy dissipation
μ	fluid dynamic viscosity
ρ	fluid density
σ	cavitation index

INTRODUCTION

Spillways are typically utilized in dams to prevent water overtopping and to reduce the risk of the ensuing dam failure (Najafzadeh *et al.* 2017). In large dams, the kinetic energy at the spillway toe is such that may it cause scouring (Bakhtyar & Barry 2009). So, the dissipation of the flow energy at the spillways' downstream is the focus of attention for the researchers. For this purpose, dissipator structures such as step, stilling basin, baffle, plunge pool, and flip bucket are employed (Farhodi *et al.* 2010; Najafzadeh 2015; Castillo *et al.* 2017; Karami Moghadam *et al.* 2019, 2020). The need to increase discharge capacity has led to the usage of nonlinear weirs (Akbari Kheir-Abadi *et al.* 2020). In the stepped spillways, the steps take action as roughness to dissipate energy. The dissipation of energy on the face of the spillway causes a great diminishing of the stilling basin's length at downstream (Babaali *et al.* 2015). Formerly, due to the long construction time and high maintenance costs for the stepped spillways, they were no longer used by the engineers and replaced by other initiatives (Mansoori *et al.* 2017). Along with the technology advancement and by introducing

the Roller Compacted Concrete method, the construction time of the spillways was shortened, and while becoming easier to maintain, the energy dissipation increased in these structures (Mansoori *et al.* 2017).

According to the researchers conducted by Khatsuria (2005), the usage of stepped spillways was constrained up to $30 \text{ m}^3/\text{s.m}$ as a result of cavitation damage at higher discharges. Modeling various horizontal, inclined, and end sill steps on the chutes with different numbers of steps, Chinnanarsi & Wongwises (2006) studied energy dissipation and its relationship with relative critical depth. Their results showed that the step with end sill has a more substantial impact on the dissipation of energy than the other two steps. Gonzalez & Chanson (2007) investigated the features of the flow passing through the stepped spillway at different chutes for earth dams. They presented new design criteria for the stepped spillways with various geometric specifications. Applying smooth and rough steps and three types of step roughness, Gonzalez *et al.* (2008) examined the effect of step roughness on the flow pattern in laboratory and measured the air-water flow attributes for several discharges. They concluded that step roughness has no impact on the flow regime. Using a physical model and studying parameters such as flow velocity, energy dissipation, and aeration inception point, Hunt & Kadavy (2010) showed that the energy loss increases linearly by 30% from zero near the crest of the dam toward the inception point. Felder & Chanson (2011) have arrived at the fact that little discrepancies are seen between the energy dissipation in the cases using uniform and nonuniform steps. Wuthrich & Chanson (2014) investigated the hydraulic function of gabion-stepped spillways with two configurations in the laboratory. Their results showed that in low discharges, the proportion of critical depth to step height less than 0.3, the nappe flow does not occur and the flow permeates merely through the space between the rocks in the gabions. Also, relative energy dissipation over flat-stepped spillway was greater than gabion-stepped spillways in transition and skimming flow regimes. Al-Shukur *et al.* (2014) used various types of step combinations like inverse inclined step, horizontal step, and step with end sill to scrutinize energy dissipation. They showed that the shape of the steps has made the most

contribution to the energy dissipation. [Thulfikar Razzak \(2015\)](#) has pointed out that the decrease in the number of steps and spillway slope may have given rise to the increase in the dissipation of energy. He also verified that the stepped spillway has more influence on energy dissipation in comparison with the flat-sloped spillway. With regard to the skimming flow, [Parsaie *et al.* \(2016\)](#) have judged that the number of drops, as well as the proportion of critical depth to the step height, is of the most effect on the dissipation of energy.

In recent decades, owing to the high expenditure of the physical models, the researchers have concentrated on the numerical methods for their precisions in the simulation of the hydraulic parameters ([Najafzadeh *et al.* 2014](#)). [Baylar *et al.* \(2011\)](#) have simulated the energy loss and the flow pattern on the stepped chutes by the numerical model. Their results proved that the flow aeration efficiency grows with the increase of energy dissipation, and the aeration of the nappe flow is more than that of the skimming flow. [Nikseresht *et al.* \(2013\)](#) employed the methods of volume of fluid (VOF) and Mixture to simulate the flow in the stepped spillways with different slopes. They inferred from their investigations that in a constant slope, any increase in discharge leads to a slump in the rate of energy dissipation. [Attarian *et al.* \(2014\)](#) engaged in the subject of energy dissipation and velocity profile using numerical simulation. Applying the Flow-3D model, [Muhammad Rezapour Tabari & Tavakoli \(2016\)](#) have utilized the flow simulation wielded on the stepped spillway to deduce that the model has a great capability in this regard. [Hamedi *et al.* \(2016\)](#) used the numerical model to study the effect of reverse slope of the step as well as sills with different heights and thickness upon relative energy dissipation and, finally, to suggest the best reverse slope and sill height. [Mansoori *et al.* \(2017\)](#) determined the flow conditions over the stepped spillway with different step geometries and with the maximum dissipation of energy.

This research aimed to evaluate the performance of the Flow-3D model in the simulation of the flow passing through the stepped spillway and to study the effects of the block barriers in these spillways on the rate of energy dissipation. Study the impacts of the block barriers as well as their optimum dimensions to maximize energy dissipation is among the innovations of the present investigation.

METHODS

Dimensional analysis

The characteristics of the fluid and the geometry of the spillway determine how the flow passes over the spillway. Equation (1) includes the parameters effective on the flow over the stepped spillway ([Parsaei *et al.* 2016](#)).

$$f(H_t, \Delta H, y_c, V, \rho, \mu, g, l, h, L_b, H_b, N) = 0 \quad (1)$$

where H_t stands for total energy of flow at the spillway's upstream, ΔH represents the energy difference between upstream and downstream, y_c is the critical depth, V designates the flow velocity at upstream, ρ is fluid density, y represents the upstream flow depth, μ is fluid dynamic viscosity, g is the gravitational acceleration, l stands for the step's length, h is the step's height, L_b represents the block's length, H_b is the height of the block, and N designates the number of steps. By using Buckingham theory, the dimension-less parameters effective on relative energy dissipation are obtained as in the following equation:

$$\frac{\Delta H}{H_t} = f\left(\frac{y_c}{h}, \frac{L_b}{l}, \frac{H_b}{h}, \frac{h}{l}, \text{Re}, \text{Fr}, N\right) \quad (2)$$

where $\Delta H/H_t$, Re, and Fr are relative energy dissipation, Reynolds Number, and Froude Number, respectively. Due to the insignificance of viscosity forces in the open channel flow, the spillway angle (or the ratio h/l) being constant, and the number of steps invariable in this research, the values of Re, h/l , and N are disregarded.

Physical model

In this research to calibrate the numerical model, the data obtained from the physical model conducted by [Heydari Orojlo *et al.* \(2011\)](#) were used. They employed a rectangular flume with dimensions of 7 m length, 0.56 m width, and 1.4 m height. To moderate the flow, a honeycomb was applied in the beginning part of the flume. The flow entered the flume from the underground tank via a pump and after passing over the stepped spillway model, a gate controls

the downstream flow depth. To measure the discharge, a triangular weir was used at the end of the secondary tank. The models of the stepped spillway were made of Plexiglass and were set 2 m away from the beginning of the flume. The stepped spillway models with a face angle of 21.8° and possessing seven steps are employed in the experiments. The height of the spillways was constant at 120 cm. The ogee parts at the upstream of the steps were designed by the USBR standard as $Y = -0.9157X^{1.873}$ (Heydari Orojlo et al. 2011). The step's length (l), step's height (h), and the ratio h/l for the model were, respectively, 33.5, 13.4, and 0.4 cm. After establishing the flow in the flume, the location where the hydraulic jump occurred was adjusted by the sluice gate. The flow depths were measured through a gauge by a ± 0.1 mm precision. The flow energy upstream and downstream of the spillway and the rate of energy dissipation were computed following the measurement of the flow depth upstream as well as before and after the hydraulic jump.

Numerical model Flow-3D

The model Flow-3D was used to numerically simulate the flow over the stepped spillway. This model can solve a wide range of problems concerning fluid flow (Lucio 2015). The method of the finite volume is used here to solve Reynolds Average Navier-Stokes equations in a Cartesian coordinate system. Flow-3D uses the function VOF to define the free surface of the flow. In this software, the construction of geometry and grid generation are two independent jobs. The base equations in CFD models such as Flow-3D include continuity equations and momentum equations known as the governing equations for the fluid dynamic. The governing equations numbered as (3) and (4) below (Flow Science Inc. 2018):

$$\frac{\partial u_i}{\partial x_i} = 0 \quad (3)$$

$$\frac{\partial u_i}{\partial t} + u_j \frac{\partial u_i}{\partial x_j} = -\frac{1}{\rho} \frac{\partial P}{\partial x_i} + \nu \left(\frac{\partial^2 u_i}{\partial x_i \partial x_j} \right) + g_i \quad (4)$$

In these equations, u_i and u_j are, respectively, the velocity components in the directions of x_i and x_j , ρ stands

for fluid density, P represents the pressure, t is the time component, ν is the kinematic viscosity, and g stands for the gravitational acceleration.

Block barriers geometry

In this research, the stepped spillway model with face angle as 21.8° , the $h/l = 0.4$, and seven steps was used. To investigate the impact of the end block dimensions on energy dissipation, the nine series of blocks with different geometries were considered. In these blocks, the ratios $L_b/l = 0.3$, 0.4, and 0.5, and the ratios $H_b/h = 0.3$, 0.4, and 0.5 were taken. To sketch the models, the AutoCad software was used. Figure 1 illustrates the parameters h , l , H_b , L_b , and the arrangement of the blocks.

The unit discharge (q) in this research was adopted to be 0.01, 0.02, 0.05, 0.07, and 0.1 m^2/s . Taking into account the values of q , H_b/h , L_b/l , along with the no-block control mode, the model was run for 50 cases.

Flow simulation

To simulate the flow pattern in the Flow-3D environment, first the geometry of each model was drawn by the AutoCad software and saved with the stl format. Afterward, each of the models was called in the Flow-3D environment for meshing and flow simulation. Calibration includes the determination of mesh sizes and the type of turbulence model.

Meshing and turbulence model

Taking a mesh having a large cell size may cause more differences between the results of the physical and numerical

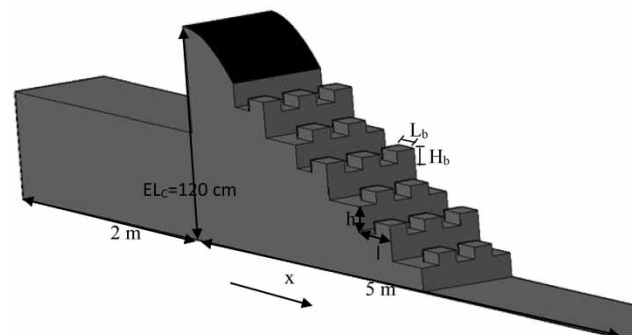


Figure 1 | Parameters h , l , H_b , L_b , and the blocks array in stepped spillway.

model, while selecting a very small cell size would lengthen the running time of the model (Lucio 2015). By selecting different mesh sizes and running the model, according to the position of the spillway model, which was located at a distance of 2 m from the beginning of the flume and also minimizing the upstream flow velocity, from the beginning of the flume to a distance of 1.6 m, cell size was selected as 1 cm. From the 1.6 m distance toward the flume's end, the cell sizes were taken to be 0.5 cm. The Flow-3D model uses different turbulence models to simulate flow turbulence. In the calibration stage to select the appropriate turbulence model, standard k- ϵ and RNG k- ϵ turbulence models were evaluated in terms of accuracy and running time.

Boundary conditions

The boundary conditions exercised in this investigation were symmetry for the upper boundary, Y_{\max} , wall for the lower, Y_{\min} , left, Z_{\max} , and right boundary, Z_{\min} , volume flow rate for the inlet, X_{\min} , and outflow for the outlet, X_{\max} (Morovati et al. 2016; Mansoori et al. 2017). The boundary conditions are shown in Figure 2. The model was run following entering the flow's attributes and determining the boundary conditions. Then, the water level and the flow depth at upstream and downstream were determined, and the relative energy dissipation rate was computed.

Relative energy dissipation

After running the Flow-3D model in each spillway mode and to ensure the flow stability, the total energy at the spillway's

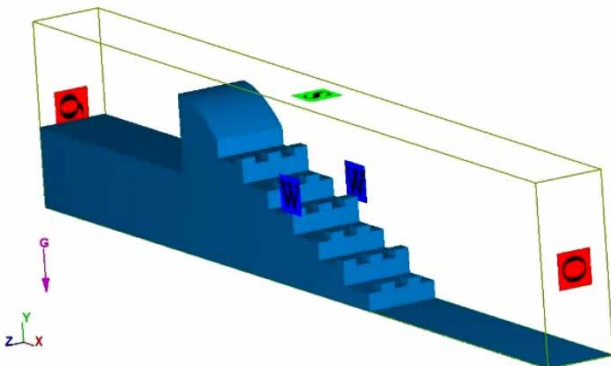


Figure 2 | Boundary conditions used in the numerical model.

upstream was computed through Equation (5) (Mansoori et al. 2017).

$$H_t = EL_c + 1.5y_c \quad (5)$$

where H_t (m) is the total energy at upstream, EL_c (m) designates the spillway's crest level at upstream proportionate to the flume's bottom at downstream, and y_c (m) represents the flow critical depth. According to the flume's cross section being rectangular, the critical depth was obtained from the following equation:

$$y_c = \left(\frac{q^2}{g} \right)^{\frac{1}{3}} \quad (6)$$

The energy at the downstream of spillway could be calculated through the following equation:

$$H_1 = y_1 + \frac{q^2}{2gy_1^2} \quad (7)$$

In which H_1 (m) stands for the energy at the spillway's toe, y_1 (m) is the primary depth of hydraulic jump, and q (m^2/s) is the unit discharge. In high discharges, in contrast to low discharge, the water depth varies across the flume due to the flow turbulence which makes its evaluation difficult. When it is the case, the sequent depth of the hydraulic jump (y_2) is determined, and with the help of Equation (8), the primary depth is obtained to be used in the computation of the flow's energy:

$$y_1 = \frac{1}{2}y_2 \left(\sqrt{1 + 8 \left(\frac{y_c}{y_2} \right)^3} - 1 \right) \quad (8)$$

After computing the energy at upstream and downstream, the amount of relative energy dissipation was calculated via the following equation:

$$\frac{\Delta H}{H_t} = \frac{(H_t - H_1)}{H_t} \times 100 \quad (9)$$

where $\Delta H/H_t$ (%) is the percentage of relative energy dissipation.

Model evaluation

The statistical indicators correlation coefficient, R^2 , and root mean square error, RMSE, were computed, respectively, by Equations (10) and (11) to be used in the evaluation of the model (Amini *et al.* 2009).

$$R^2 = \frac{\left[\sum_{i=1}^n (P_i - \bar{P})(O_i - \bar{O}) \right]^2}{\sum_{i=1}^n (P_i - \bar{P})^2 \sum_{i=1}^n (O_i - \bar{O})^2} \quad (10)$$

$$\text{RMSE} = \sqrt{\frac{1}{n} \sum_{i=1}^n (P_i - O_i)^2} \quad (11)$$

In these equations, n , P_i , O_i , \bar{P} , and \bar{O} are, respectively, the number of data, the amount of energy dissipation in model Flow-3D, the energy dissipation rate in the physical model, the average dissipation of energy in Flow-3D, and that in the physical model. For reliability analysis, statistical indicators R^2 , slopes K and K' were used. Slopes K and K' were calculated as follows (Homaei & Najafzadeh 2020; Najafzadeh & Oliveto 2020):

$$K = \frac{\sum_{i=1}^n O_i \times P_i}{\sum_{i=1}^n P_i^2} \quad (12)$$

$$K' = \frac{\sum_{i=1}^n O_i \times P_i}{\sum_{i=1}^n O_i^2} \quad (13)$$

Model will be considered acceptable if it satisfied following conditions: $R^2 > 0.6$, $0.85 \leq K \leq 1.15$ or $0.85 \leq K' \leq 1.15$ (Tropsha *et al.* 2003).

Cavitation

One of the important phenomena in spillways design is cavitation phenomenon. To investigate the possibility of cavitation, cavitation index (σ) is used (Frizell *et al.* 2013):

$$\sigma = \frac{P_0 - P_v}{\rho \frac{V_0^2}{2}} \quad (14)$$

where P_0 (N/m²) is the absolute pressure at the desired point of flow, P_v (N/m²) is the absolute pressure of water vapor, ρ (kg/m³) is water density, and V_0 (m/s) is the flow velocity. For $\sigma > 0.2$, there is a possibility of cavitation on spillways (Frizell *et al.* 2013).

RESULTS

Model validation

Since the physical experiments were carried out on the 21.8° stepped spillway in the no-block situation, the simulation of the flow passing over the spillway was performed in the conditions similar to those of the physical model before comparing the results. Table 1 and Figure 3 show the comparison between the energy dissipation in the physical as well as numerical models in the no-block case.

To choose an appropriate turbulent model, the standard $k-\epsilon$ and RNG $k-\epsilon$ models were examined. The results indicated that as regards precision, both models acted almost the same. The R^2 and RMSE were calculated 0.77 and 6.30 for standard $k-\epsilon$ model and 0.84 and 6 for RNG $k-\epsilon$ model, respectively. When it comes to run time, however, RNG $k-\epsilon$ lasted somewhat shorter and whence it was selected for simulation. Amini & Parto (2017) and Morovati *et al.* (2016) also have confirmed the superiority of this

Table 1 | The amount of relative energy dissipation in physical and numerical models and statistical measures

		q (m ² /s)					R^2	RMSE	K	K'
		0.01	0.02	0.03	0.04	0.05				
Energy dissipation (%)	Experimental	86	83.3	80.67	82.33	79.3				
	Numerical (RNG $k-\epsilon$)	93.93	91.35	86	85	83.46	0.84	6	0.93	1.07
	Numerical ($k-\epsilon$)	94	91.40	87	84.8	84.10	0.77	6.30	0.93	1.07

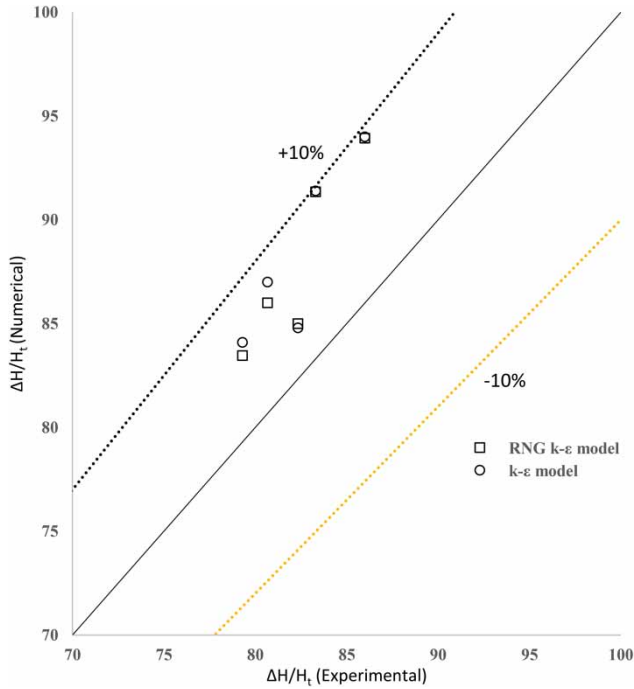


Figure 3 | Energy dissipation in physical versus numerical models.

turbulence model. Table 1 and Figure 3 acknowledge that the numerical model estimates the energy dissipation from 3.5 to 10% more than the physical model does. The indicators R^2 and RMSE applied to the outcomes of the two models also guarantee that the results of the numerical model well agree with those of the physical one. The results are in compliance with what was pointed out by Mohammad Rezapour Tabari & Tavakoli (2016) about the accuracy of the numerical models. Reliability analysis demonstrates that $R^2 > 0.6$ and both K and K' are between 0.85 and 1.15 indicating a relatively high predictive ability of Flow-3D model for energy dissipation estimation.

Flow pattern on spillway

The three flow regimes, that is, nappe flow, transition flow, and skimming flow, are likely to be taking place over the stepped spillway. The conversion threshold of these flow regimes has been among the topics of interest to some researchers. In this research, the simulation of the flow pattern was rendered using the turbulence RNG k-ε model and relying on the Flow-3D model for different situations.

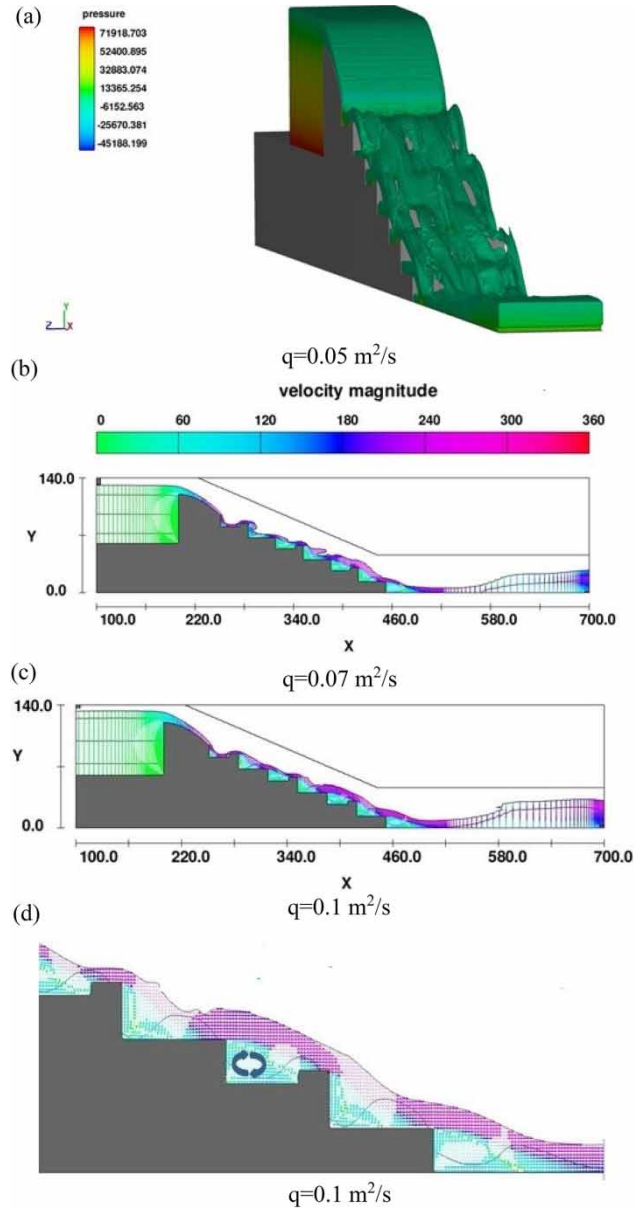


Figure 4 | Flow simulation with $L_b/l = H_b/h = 0.3$: (a) $q = 0.05 \text{ m}^2/\text{s}$; (b) $q = 0.07 \text{ m}^2/\text{s}$; (c) $q = 0.1 \text{ m}^2/\text{s}$ and (d) vortices behind the blocks in $q = 0.1 \text{ m}^2/\text{s}$.

Figure 4, for instance, shows the results pertaining to flow simulation over the stepped spillway for the ratios $L_b/l = H_b/h = 0.3$ and for three unit discharges as 0.05, 0.07, and $0.1 \text{ m}^2/\text{s}$. The flow pattern and vortices behind the blocks are also shown in Figure 4.

Figure 4(a) corresponds to the unit discharge $0.05 \text{ m}^2/\text{s}$ and $y_c/h = 0.47$. As observed, for this ratio the flow is still of the napped type. In Figure 4(b) and 4(c), the increase in

discharge makes a flow-type conversion from nappe to skimming. By virtue of the relation of Chanson (1994), the upper limit for the conversion of these two flow regimes when $h/l = 0.4$ is $y_c/h = 0.73$. Figure 4(c), which is related to the unit discharge $0.1 \text{ m}^2/\text{s}$ and $y_c/h = 0.75$, shows that the flow is not yet completely converted to the skimming flow. This indicated that the block over the spillway causes a delay in the regime conversion from nappe into skimming. Lastly, Figure 4(d) depicts the vectors of velocity and vortices behind the blocks. The comparison between the vortices over two consecutive steps indicates that the presence of the blocks further increases this type of flow followed by more energy dissipation.

Block height

Figure 5 illustrates the alterations in the relative energy dissipation, $\Delta H/H_t$, versus y_c/h for three different ratios of the block's height to the step's height, H_b/h , as 0.3, 0.4, and 0.5 and also with the no-block conditions. These changes are sketched for three ratios of $L_b/l = 0.3, 0.4, \text{ and } 0.5$.

As shown in Figure 5, with the increase in the value of y_c/h , the relative energy dissipation decreases in all block's height ratios. This is in conformity with the results obtained by Al-Shukur et al. (2014) and Morovati et al. (2016).

For all L_b/l , the block barriers have made growth in the dissipation of energy. In cases when the y_c/h is low (i.e. in low discharges), the block barriers have not been of so many effects on the increase of energy dissipation. Indeed, in low discharges, the flow is completely of nappe type and after the chute from the upper to the lower steps, the flow strikes the blocks at low velocity and therefore the blocks could not make noteworthy contributions to reducing the flow velocity rate. As y_c/h increases (discharge increasing), the relative energy dissipation increases more in the block mode than in the case without blocks which proves the salutary effect of the blocks upon energy dissipation. For all L_b/l ratios in low discharges, the impact of the blocks with different heights on energy dissipation is almost the same and the effect of the blocks' heights more turns up with an increase in discharge. When $L_b/l = 0.3$, Figure 5(a) shows the most energy dissipation rate with $H_b/h = 0.3$ to be 91% on average, and the least rate as 88% on average with the height ratio $H_b/h = 0.5$. In the block mode with $H_b/h = 0.3, 0.4, \text{ and } 0.5$, the energy dissipation has climbed, respectively, by 8.6, 7.4, and 5.8% compared with the no-block mode.

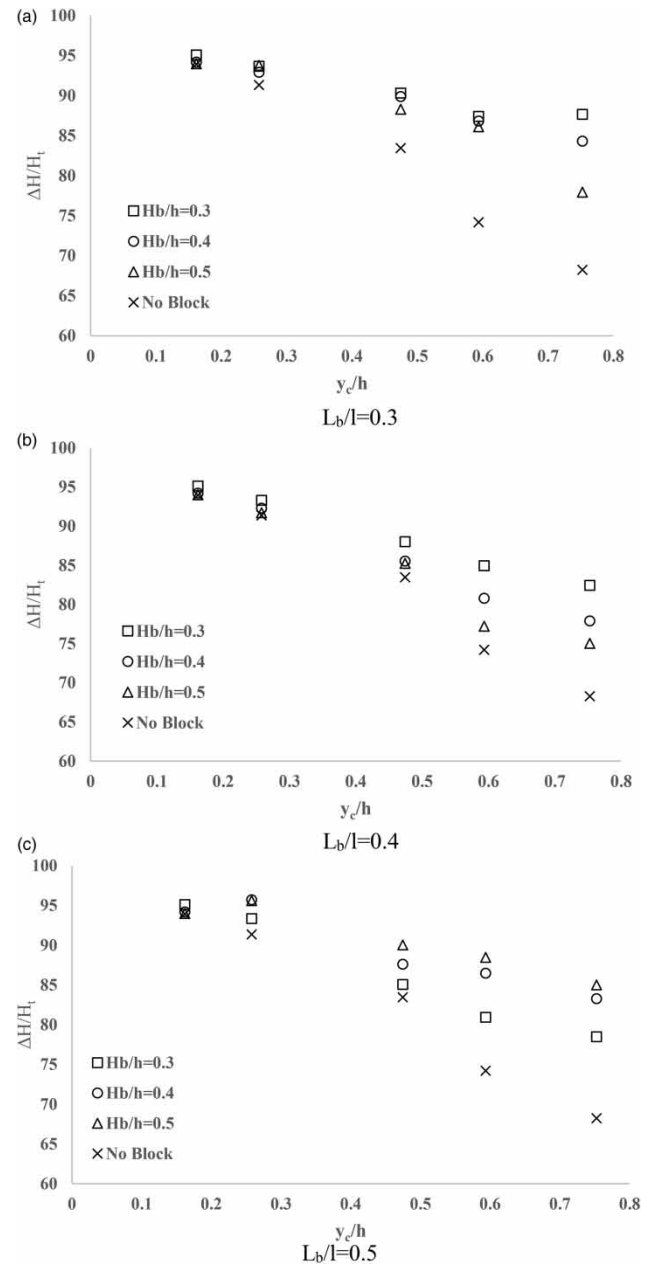


Figure 5 | Effect of block's height in energy dissipation: (a) $L_b/l = 0.3$; (b) $L_b/l = 0.4$; (c) $L_b/l = 0.5$.

0.5, the energy dissipation has climbed, respectively, by 8.6, 7.4, and 5.8% compared with the no-block mode.

In Figure 5(b) for $L_b/l = 0.4$, the dissipation of energy takes its maximum at $H_b/h = 0.3$ and its minimum at $H_b/h = 0.5$. Incidentally, at the three height ratios $H_b/h = 0.3, 0.4, \text{ and } 0.5$, the energy dissipation rate has increased, respectively, by 6.5, 3.9, and 2.4% relative to the no-block

situation. In the maximum ratio $y_c/h = 0.75$, the energy dissipation rate is 68% in the no-block case, and in the presence of the blocks with three height ratios of 0.3, 0.4, and 0.5 it reaches 82, 78, and 75%, respectively.

In Figure 5(c) and for $L_b/l = 0.5$, contrary to the other two ratios, the energy dissipation grows along with the increase in the blocks' heights. In this case, the rate of energy dissipation at the ratio $H_b/h = 0.5$ is greater than the cases when $H_b/h = 0.3$ and $H_b/h = 0.4$. Besides, at the three height ratios $H_b/h = 0.3, 0.4,$ and 0.5 , the rate of relative energy dissipation is greater than that in the no-block mode by 4.35, 7.22, and 8.38%, respectively. So, one could declare that at the length ratios $L_b/l = 0.3$ and 0.4 , the blocks of fewer heights are more contributory in energy dissipation, and at $L_b/l = 0.5$, the increase in the height ratio brings about a rise in the rate of energy dissipation. Keshavarz-Eskandari & Esmaili-Varaki (2019) also have realized that for a set block length, the dissipation of energy increases with the rise in the blocks' heights.

Block length

Figure 6 illustrates the changes in the relative energy dissipation, $\Delta H/H_i$, versus y_c/h for proportions of the block's length to the step's length, L_b/l , equal to 0.3, 0.4, and 0.5, together with the no-block conditions. The changes are drawn for three ratios as $H_b/h = 0.3, 0.4,$ and 0.5 .

Figure 6 shows that at all ratios of H_b/h , the rise in y_c/h caused a decrease in the energy dissipation rate. Also, the effect of the blocks, as well as the length ratio in low discharges, is insignificant in the growth of energy dissipation though the effect escalates along with the increase in discharge. Figure 6(a) demonstrates that when $H_b/h = 0.3$, the rate of relative energy dissipation takes its maximum at the ratio $L_b/l = 0.3$ and it has the smallest amount at $L_b/l = 0.5$. On average, the relative energy dissipation at the $L_b/l = 0.3, 0.4,$ and 0.5 increased compared with the no-block mode by, respectively, 8.6, 6.5, and 4.5%. At $y_c/h = 0.75$ where the blocks are of the most influence in the increase of energy dissipation, the rate of dissipation was 68% in the no-block case, and at $L_b/l = 0.3, 0.4,$ and 0.5 the respective percentages were 87.7, 82.4, and 78.5%. As for the height ratio of $H_b/h = 0.4$, Figure 6(b) bears evidence that the energy dissipation rates at the length ratios

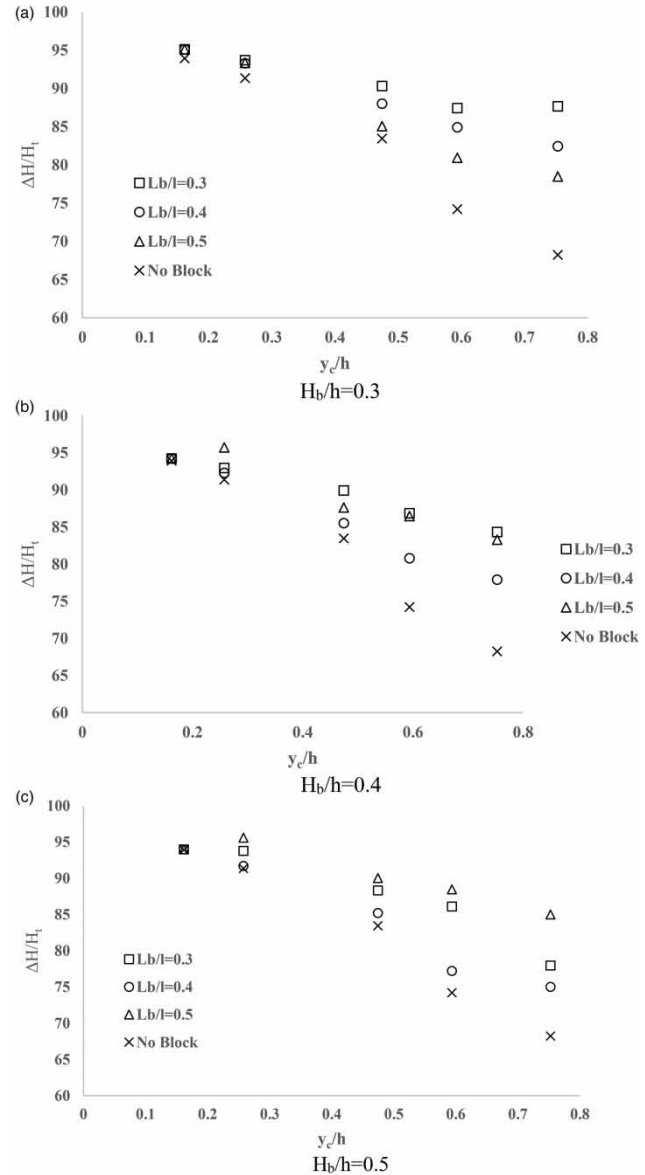


Figure 6 | Effects of the blocks' lengths on the relative energy dissipation: (a) $H_b/h = 0.3$; (b) $H_b/h = 0.4$ and (c) $H_b/h = 0.5$.

$L_b/l = 0.3$ and $L_b/l = 0.5$ are close to each other and are both greater than the rate at $L_b/l = 0.4$. More precisely, the energy dissipation rates at $L_b/l = 0.3$ and $L_b/l = 0.5$ are, respectively, 3.5 and 3.3% more than those for $L_b/l = 0.4$.

According to Figure 6(c) which corresponds to $H_b/h = 0.5$, the dissipation of energy gets the peak when $L_b/l = 0.5$ and attains its minimum when $L_b/l = 0.4$. At this height ratio, the energy dissipation has increased relative to the no-block mode whenever $L_b/l = 0.3, 0.4,$ and 0.5 with the

respective increase percentages of 5.8, 2.4, and 8.4%. It is, therefore, concluded that at low height ratios the shorter blocks and at great height ratios the lengthier blocks had the most contributions in the energy dissipation when compared with the no-block situation. Figure 7 shows the comparison between the relative energy dissipation among the nine series of blocks.

Figure 7 shows that both the blocks with $H_b/h = 0.3$ and $L_b/l = 0.3$ and those with $H_b/h = 0.5$ and $L_b/l = 0.5$ were assigned the most increase in energy dissipation, and the series of blocks with $H_b/h = 0.3$ and $L_b/l = 0.4$ had the least rate when compared with the no-block case.

Cavitation

Figure 8 shows the cavitation index in the states of with and without block barriers with the ratios of $L_b/l = 0.3$ and $H_b/h = 0.3$, and for the unit discharge of 0.02, 0.05, 0.07, and 0.1 m²/s, where X is the distance from the beginning of the flume.

As shown in Figure 8, with increasing discharge, the cavitation index increases. Consequently, the probability of cavitation decreases. In both cases, without block and with block barriers, in the ogee part of the spillway, $X = 2-2.5$, the cavitation index is less than 0.2. However, in most steps, this index is higher than the critical value which indicates that cavitation is more likely to occur in smooth spillways than in stepped ones. This result is consistent with the findings of Frizell et al. (2013).

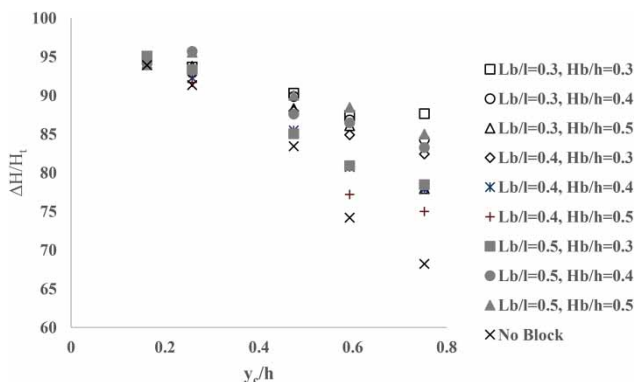


Figure 7 | Relative energy dissipations at different length and height ratios of blocks.

DISCUSSION

Figure 9 represents a comparison between the results of energy dissipation on the stepped spillway obtained in this research at blocks with $H_b/h = 0.5$ and $L_b/l = 0.5$ and in the no-block mode and those given by Al-Shukur et al. (2014), Naderi Rad et al. (2009), and Keshavarz-Eskandari & Esmaeili-Varaki (2019).

Al-Shukur et al. (2014) conducted their experiments on the stepped spillways with $h/l = 0.84$ while taking the step's height equal to the height of the rectangular end sill, $H_b/h = 1$. They carried out their researches for two cases. In the first case, the sill was put at the ends of all the steps (A_1 in Figure 9), and in the second case, the end sills were put in between two steps (A_2 in Figure 9).

The experiments of Naderi Rad et al. (2009) on the stepped spillway were performed with $h/l = 1$ along with three height ratios as $H_b/h = 0.2, 0.4, \text{ and } 0.6$ while utilizing flat end sills. Keshavarz-Eskandari & Esmaeili-Varaki (2019) adopted the ratio $h/l = 0.5$ and used blocks with various length and height ratios. Similar to that is reported in the previous researches and as discerned in Figure 9 in the current study, the relative energy dissipation decreases with the increase in the y_c/h ratio. Also, applying block or end sill is conducive to the increase in energy dissipation. In the investigation done by Al-Shukur et al. (2014), the amounts of energy dissipation for two arrangements A_1 and A_2 are not so different. The amount of relative dissipation of energy in the present research in the no-block case exceeds that in the work of Naderi Rad et al. (2009) in the no-sill condition which is due to the less spillway's angle (the less value of h/l) in current research. The results obtained by Heydari Orojlo et al. (2011) and Thulfikar Razzak (2015) attest that the reduction of the spillway's angle causes an increase in the energy dissipation. Also, Naderi Rad et al. (2009) held that the relative energy dissipation grows with the increase in the height ratio of the end sill. This result agrees with the achievements of the current study and those of Keshavarz-Eskandari & Esmaeili-Varaki (2019) concerning block barriers. In the block mode with the ratios of $H_b/h = 0.5$ and $L_b/l = 0.5$, the relative energy dissipation rate acquired in the present research goes beyond that given by Keshavarz-Eskandari & Esmaeili-Varaki (2019) on account of the difference in the location of the blocks. In

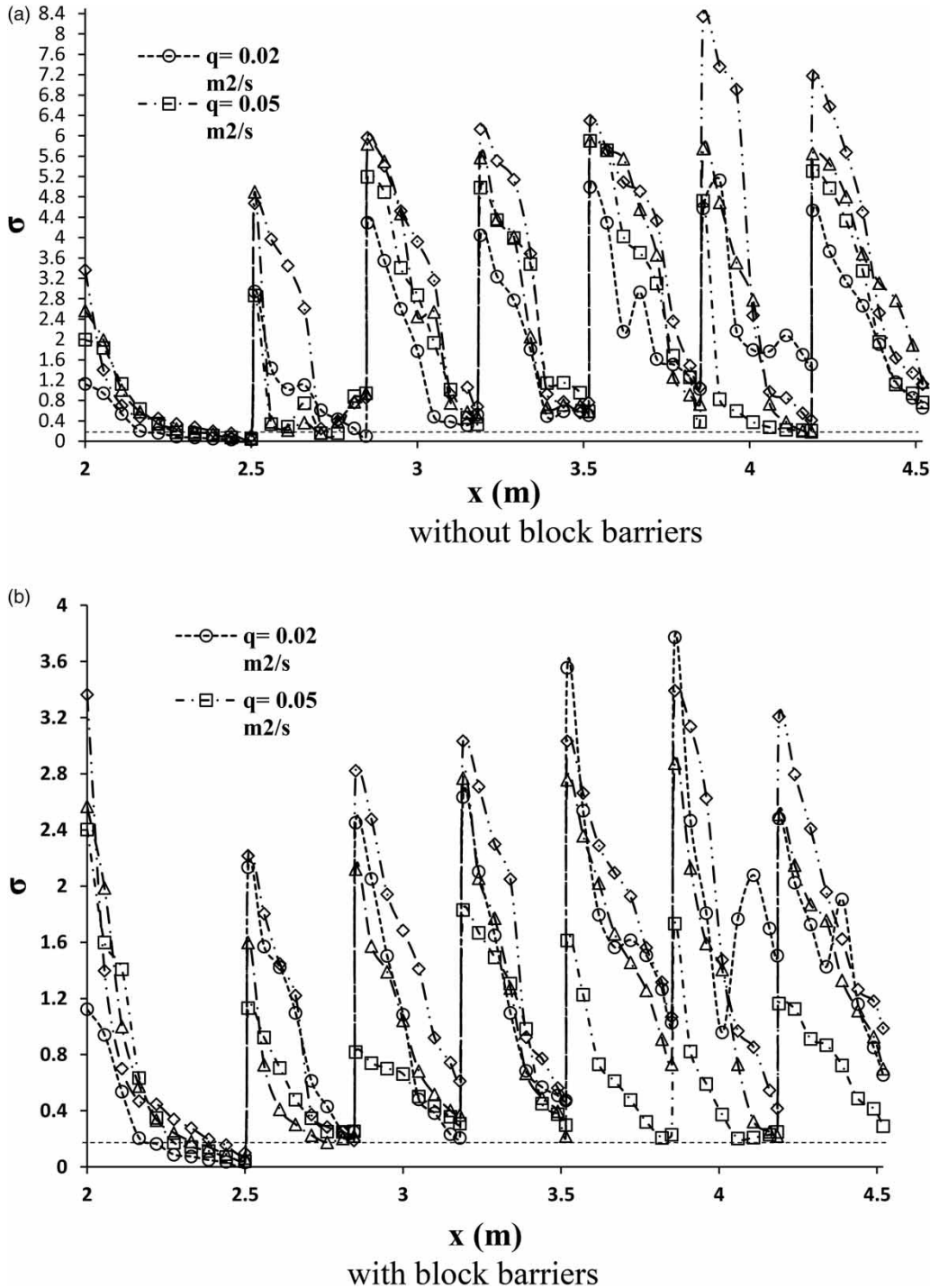


Figure 8 | Cavitation index for stepped spillway: (a) without block barriers and (b) with block barriers.

fact, their results pertain to the case where the blocks are set at the beginning of the steps rather than locating at their ends. So, the location of the blocks could be also a key

factor in the dissipation of energy. Other researchers have continued their experiments for higher ratios y_c/h though the energy dissipation trend in this research when this

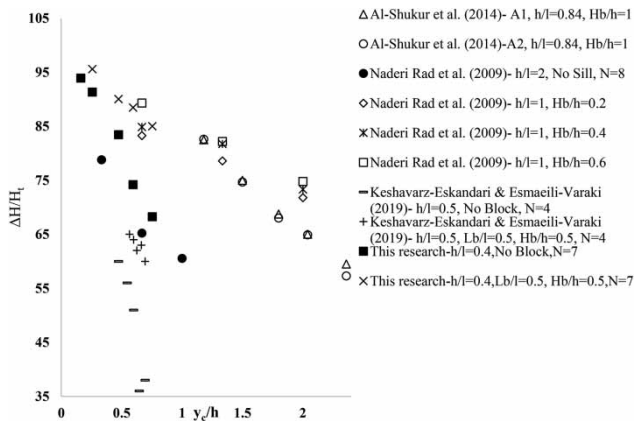


Figure 9 | Comparison between the results of the present research and the previous ones.

ratio increase is well in accord with the others' achievements. This comparison shows that blocks and sills have almost the same effects on the increase of energy dissipation. However, future investigations in the same and analogous conditions may shed more light on the subject.

CONCLUSIONS

In this research, the effects of height and length of the block on the rate of energy dissipation in the 21.8° stepped spillway were studied using the Flow-3D model. All the spillway models possessed seven steps, and the blocks involving nine different geometries concerned the ratios H_b/h and $L_b/l = 0.3, 0.4,$ and 0.5 . The most important results of the current research are as follows:

- The comparison between the results of the laboratory model and the numerical model represents the efficiency of the Flow-3D in flow simulation and estimation of energy dissipation in stepped spillways.
- The increase in discharge is a leading factor in the decline of energy dissipation and in supporting the effect of the blocks' geometry in this respect.
- In contrast to the $L_b/l = 0.3$ and $L_b/l = 0.4$, the increase of the height ratio in the case of $L_b/l = 0.5$ makes an increase of relative energy dissipation.
- The blocks with the ratios $H_b/h = L_b/l$ equal to 0.3 and 0.5 with respective percentages 8.6 and 8.4% applied the most effects on dissipation. The shorter blocks in

low height ratios and the lengthy blocks in greater height ratios were responsible for the most energy dissipation.

DATA AVAILABILITY STATEMENT

All relevant data are included in the paper or its Supplementary Information.

REFERENCES

- Akbari Kheir-Abadi, M., Karami Moghadam, M., Sabzevari, T. & Ghadampour, Z. 2020 An experimental study of the effects of the parapet walls geometry on the discharge coefficient of trapezoidal piano key weirs. *Flow Measurement and Instrumentation* **73** (2020), 101742. <https://doi.org/10.1016/j.flowmeasinst.2020.101742>.
- Al-Shukur, A. K., Al-Khalaf, S. K. & Al-sharifi, I. M. 2014 Flow characteristics and energy dissipation losses in different configurations of steps of stepped spillway. *International Journal of Innovative Research in Science, Engineering and Technology* **3** (1), 8823–8832.
- Amini, A. & Parto, A. A. 2017 3D numerical simulation of flow field around twin piles. *Acta Geophysica* **65**, 1243–1251. <https://doi.org/10.1007/s11600-017-0094-x>.
- Amini, A., Ali, T. M., Ghazali, A. H. B. & Huat, B. K. 2009 Adjustment of peak streamflows of a tropical river for urbanization. *American Journal of Environmental Sciences* **5** (3), 285–294. doi:10.3844/ajessp.2009.285.294.
- Attarian, A., Hosseini, K. H., Abdi, H. & Hosseini, M. 2014 The effect of the step height on energy dissipation in stepped spillways using numerical simulation. *Arabian Journal for Science and Engineering* **39** (4), 2587–2594. <https://doi.org/10.1007/s13369-013-0900-y>.
- Babaali, H., Shamsai, A. & Vosoughifar, H. 2015 Computational modeling of the hydraulic jump in the stilling basin with convergence walls using CFD codes. *Arabian Journal for Science and Engineering* **40** (2), 381–395. <https://doi.org/10.1007/s13369-014-1466-z>.
- Bakhtyar, R. & Barry, D. A. 2009 Optimization of cascade stilling basins using GA and PSO approaches. *Journal of Hydroinformatics* **11** (2), 119–132. <https://doi.org/10.2166/hydro.2009.046>.
- Baylar, A., Unsal, M. & Ozkan, F. 2011 The effect of flow patterns and energy dissipation over stepped chutes on aeration efficiency. *KSCE Journal of Civil Engineering* **15** (8), 1329–1334. <https://doi.org/10.1007/s12205-011-1360-0>.
- Castillo, L. G., Carrillo, J. M. & Bombardelli, F. A. 2017 Distribution of mean flow and turbulence statistics in plunge

- pools. *Journal of Hydroinformatics* **19** (2), 173–190. <https://doi.org/10.2166/hydro.2016.044>.
- Chanson, H. 1994 Comparison of energy dissipation between nappe and skimming flow regimes on stepped chutes. *Journal of Hydraulic Research* **32** (2), 213–218. <https://doi.org/10.1080/00221686.1994.10750036>.
- Chinnarasri, C. & Wongwises, S. 2006 Flow patterns and energy dissipation over various stepped chutes. *Journal of Irrigation and Drainage Engineering* **132** (1), 70–76. [https://doi.org/10.1061/\(ASCE\)0733-9437\(2006\)132:1\(70\)](https://doi.org/10.1061/(ASCE)0733-9437(2006)132:1(70)).
- Farhoudi, J., Hosseini, S. M. & Sedghi-Asl, M. 2010 Application of neuro-fuzzy model to estimate the characteristics of local scour downstream of stilling basins. *Journal of Hydroinformatics* **12** (2), 201–211. <https://doi.org/10.2166/hydro.2009.069>.
- Felder, S. & Chanson, H. 2011 Energy dissipation down a stepped spillway with nonuniform step heights. *Journal of Hydraulic Engineering* **37** (11), 1543–1548. [https://doi.org/10.1061/\(ASCE\)HY.1943-7900.0000455](https://doi.org/10.1061/(ASCE)HY.1943-7900.0000455).
- FLOW-3D® Version 12.0 User's Manual 2018 *FLOW-3D* [Computer software]. Santa Fe, NM: Flow Science, Inc. Available from: <https://www.flow3d.com>.
- Frizell, K. W., Renna, F. M. & Matos, J. 2013 Cavitation potential of flow on stepped spillways. *Journal of Hydraulic Engineering* **139** (6), 630–636. [https://doi.org/10.1061/\(ASCE\)HY.1943-7900.0000715](https://doi.org/10.1061/(ASCE)HY.1943-7900.0000715).
- Gonzalez, C. A. & Chanson, H. 2007 Hydraulic design of stepped spillways and downstream energy dissipaters for embankment dams. *Dam Engineering* **17** (4), 223–244.
- Gonzalez, C. A., Takahashi, M. & Chanson, H. 2008 An experimental study of effects of step roughness in skimming flows on stepped chutes. *Journal of Hydraulic Research* **46** (1), 24–35. <https://doi.org/10.1080/00221686.2008.9521937>.
- Hamed, A. M., Hajigholizadeh, M. & Mansoori, A. 2016 Flow simulation and energy loss estimation in the Nappe flow regime of stepped spillways with inclined steps and end sill: a numerical approach. *Civil Engineering Journal* **2** (9), 426–437. doi:10.28991/cej-2016-00000047.
- Heydari Orojlo, S., Mousavi Jahromi, S. H. & Adib, A. 2011 Influence of the steeped spillway slope on the number of optimal steps. *Journal of Irrigation Sciences and Engineering* **33** (2), 127–140. doi:10.22055/JISE.2010.13484 (In Persian).
- Homaei, F. & Najafzadeh, M. 2020 A reliability-based probabilistic evaluation of the wave-induced scour depth around marine structure piles. *Ocean Engineering* **196**, 106818. <https://doi.org/10.1016/j.oceaneng.2019.106818>.
- Hunt, S. L. & Kadavy, K. C. 2010 Energy dissipation on flat-sloped stepped spillway: part 1. Upstream of the inception point. *Transactions of the ASABE* **53** (1), 103–109. doi:10.13031/2013.29506.
- Karami Moghadam, M., Amini, A., Malek, M. A., Mohammad, T. & Hoseini, H. 2019 Physical modeling of Ski-Jump spillway to evaluate dynamic pressure. *Water* **11** (8), 1687. <https://doi.org/10.3390/w11081687>.
- Karami Moghadam, M., Amini, A. & Hoseini, H. 2020 Experimental evidence dynamic pressures reduction on plunge pool floors downstream flip bucket for increasing downstream face slopes. *Water Science and Technology-Water Supply* **20** (5), 1834–1846. <https://doi.org/10.2166/ws.2020.091>.
- Keshavarz-Eskandari, M. & Esmaeili-Varaki, M. 2019 Experimental investigation of energy dissipation over stepped-Labyrinth weirs. *Irrigation and Drainage Structures Engineering Research* **20** (74), 59–74 (In Persian). doi:10.22092/IDSER.2018.115952.1267.
- Khatsuria, R. M. 2005 Ogee or overflow spillways. In: *Hydraulics of Spillways and Energy Dissipaters* (M. D. Meyer, ed.). Marcel Dekker, New York, pp. 41–62.
- Lucio, I. 2015 *Numerical Modeling of Skimming Flow Over Stepped Spillways: Application on Small Embankment Dams*. M.Sc. Thesis, Instituto Superior Técnico, Lisboa, Portugal.
- Mansoori, A., Erfanian, S. H. & Khamchin Moghadam, F. 2017 A study of the conditions of energy dissipation in stepped spillway with A-shaped step using FLOW-3D. *Civil Engineering Journal* **3** (10), 856–867. <http://dx.doi.org/10.28991/cej-030920>.
- Mohammad Rezapour Tabari, M. & Tavakoli, S. 2016 Effects of stepped spillway geometry on flow pattern and energy dissipation. *Arabian Journal for Science and Engineering* **41** (4), 1215–1224. <https://doi.org/10.1007/s13369-015-1874-8>.
- Morovati, K., Eghbalzadeh, A. & Soori, S. 2016 Study of energy dissipation of pooled stepped spillways. *Civil Engineering Journal* **2** (5), 208–220. doi:10.28991/cej-2016-00000027.
- Naderi Rad, I., Talebbeydokhti, N. & Nikseresht, A. H. 2009 An investigation of energy dissipation in various types of stepped spillways including simple, inclined step, and steps with end sills by numerical model. *Journal of Civil and Environmental Engineering University of Tabriz* **39** (1), 53–66 (In Persian).
- Najafzadeh, M. 2015 Neuro-fuzzy GMDH based particle swarm optimization for prediction of scour depth at downstream of grade control structures. *Engineering Science and Technology, an International Journal* **18** (1), 42–51. <https://doi.org/10.1016/j.jestch.2014.09.002>.
- Najafzadeh, M. & Oliveto, G. 2020 Riprap incipient motion for overtopping flows with machine learning models. *Journal of Hydroinformatics* **22** (4), 749–767. <https://doi.org/10.2166/hydro.2020.129>.
- Najafzadeh, M., Barani, G. & Hessami-Kermani, M. 2014 Group method of data handling to predict scour at downstream of a ski-jump bucket spillway. *Earth Science Informatics* **7** (4), 231–248. <https://doi.org/10.1007/s12145-013-0140-4>.
- Najafzadeh, M., Tafarjnoruz, A. & Lim, S. Y. 2017 Prediction of local scour depth downstream of sluice gates using data-driven models. *ISH Journal of Hydraulic Engineering* **23** (2), 195–202. <https://doi.org/10.1080/09715010.2017.1286614>.
- Nikseresht, A. H., Talebbeydokhti, N. & Rezaei, M. J. 2013 Numerical simulation of two-phase flow on step-pool spillways. *Scientia Iranica, Transactions A: Civil Engineering* **20** (2), 222–230. <https://doi.org/10.1016/j.scient.2012.11.013>.

- Parsaie, A., Haghiabi, A. H., Saneie, M. & Torabi, H. 2016 Prediction of energy dissipation on the stepped spillway using the multivariate adaptive regression splines. *ISH Journal of Hydraulic Engineering* **22** (3), 281–292. <https://doi.org/10.1080/09715010.2016.1201782>.
- Thulfikar Razzak, A. 2015 Experimental study of increasing energy dissipation on stepped spillway. *Journal of Kerbala University* **13** (3), 87–100.
- Tropsha, A., Gramatica, P. & Gombar, V. K. 2003 The importance of being earnest: validation is the absolute essential for successful application and interpretation of QSPR models. *QSAR & Combinatorial Science* **22** (1), 69–77. <https://doi.org/10.1002/qsar.200390007>.
- Wuthrich, D. & Chanson, H. 2014 Hydraulics, air entrainment and energy dissipation on gabion stepped weirs. *Journal of Hydraulic Engineering* **140** (9), 04014046. [https://doi.org/10.1061/\(ASCE\)HY.1943-7900.0000919](https://doi.org/10.1061/(ASCE)HY.1943-7900.0000919).

First received 12 September 2020; accepted in revised form 30 November 2020. Available online 15 December 2020